Gas Processing Journal

Vol. 1 No. 1, January 2013
ISSN (Print): 2322-3251
PP. 70-87

The Indication of Two-Phase Flow Pattern and Slug Characteristics in a Pipeline Using CFD Method

Rahbar Rahimi*, Elahe Bahramifar and Maryam Mazarei Sotoodeh

Department of Chemical Engineering, University of Sistan and Baluchestan, Iran

(Received: 20 May 2012, Accepted: 11 November 2012)

Abstract: *Multiphase flows are commonly encountered in oil and gas industries. The transport of multiphase flow causes the formation of slug, the increase of pressure drop and the possibility of phase changes; therefore, a set of simulation runs was performed to predict flow regimes in a horizontal pipeline, and the results were compared with the Baker chart. The effects of small downward inclinations of pipelines on the formation of slugs were also considered.Volume of Fluid model (VOF) has been used to predict the flow regimes in a horizontal pipeline within an 8-cm diameter and 7-m length pipe. In order to identify the critical parameters of slug flow (mean slug frequency, slug translational velocity, hold up and pressure drop), the simulations were carried out in a 7.63-cm diameter and 5-m length pipe mounted with three different inclination angles of 0°,-0.5° and -0.8°. A good agreement between CFD model and experimental data has shown the advantage of VOF model for studying two-phase flows.*

Keywords: *Pipe Inclination, Slug Flow, CFD, VOF, Baker Chart, Two-Phase Flow*

1. Introduction

Flow fields in chemical process unit operations are complex and often include multiphase flows. The prediction of pressure gradients, liquid hold up and flow patterns occurring during the simultaneous flow of gas and liquid in pipes is necessary in designing petroleum and chemical plants (Brill & Beggs, 1994). Baker was the researcher who acknowledged the importance of flow patterns for the calculation of pressure drop, heat and mass transfer, etc., in tubes. He published the earliest flow pattern map for horizontal flow in a pipe. Baker chart shows seven different flow regimes which are mentioned below (Sandra, Heyderickx, & Marin, 2008):

* **Corresponding Author.** University of Sistan and Baluchestan, P .O.Box.98164-161, Zahedan, Iran

Authors' Email Address: Rahimi{rahimi@hamoon.usb.ac.ir}, Bahramifar{elahebahramifar@gmail.com}, Mazaheri{maryam.mazarei@gmail.com}

1. Stratified flow: At low liquid and gas velocities, a complete separation of the two phases is observed. The two phases are clearly separated by an undisturbed horizontal interface, with the liquid flowing over the bottom of the tube (under normal gravity conditions).

2. Wavy flow: When the gas velocity is increased under stratified flow conditions, waves are formed on the liquid–gas interface. These waves travel in the flow direction. The amplitude of the waves depends on the relative velocity between the phases and the properties of fluids, such as their density and surface tension.

3. Plug flow: This flow pattern is an intermittent flow that occurs at low gas flow rates and moderate liquid rates. In this regime, liquid plugs, free of entrained gas bubbles, are separated by zones of elongated gas bubbles. The diameters of the elongated bubbles are smaller than the tube diameter. As a result, there is a continuous liquid phase along the bottom of the tube below the elongated bubbles. Plug flow is also referred to as elongated bubble flow.

4. Slug flow: When the gas velocity is increased under plug flow conditions, the liquid slugs become more chaotic as compared to plug flow and the interface between the liquid slugs and the elongated gas bubbles becomes less sharp.

5. Annular flow: Higher gas flow rates will cause the liquid to form a continuous film around the perimeter of the tube. The film at the bottom of the tube may be much thicker than the film at the top (the thickness variation depends on the velocity of the gas). The interface between the liquid annulus and the gas core is disturbed by small amplitude waves. Liquid droplets can possibly be dispersed in the gas core.

6. Bubble flow: Gas bubbles are dispersed in the continuous liquid flow.

7. Spray flow: Discrete liquid droplets are dispersed in the continuous gas phase (Sandra, Heyderickx, & Marin, 2008).

The Baker flow regime map appears in Fig. 1. The quantities λ and ψ, as given by equation 1, are empirical parameters to make transition lines for systems other than air-water ones and coincide with those for an air-water system. Baker chart could be used for any combination of gas/vapor-liquid flow. For the air-water flow, λ and ψ are equal to one.

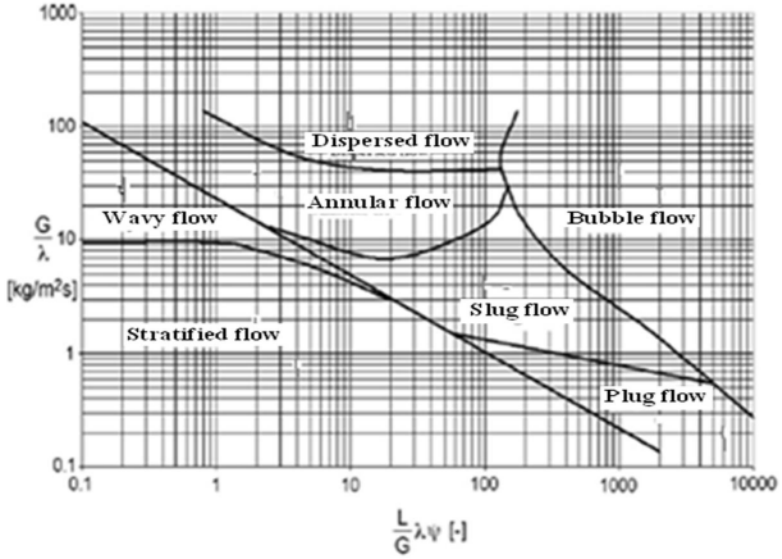

Fig. 1. Baker chart (Sandra, Heyderickx, & Marin, 2008)

$$\lambda = \left[\left(\frac{\rho_G}{\rho_A} \right) \left(\frac{\rho_L}{\rho_W} \right) \right]^{0.5} \qquad (1)$$

$$\psi = \frac{\sigma_W}{\sigma} \left[\left(\frac{\mu_L}{\mu_W} \right) \left(\frac{\rho_W}{\rho_L} \right)^2 \right]^{1/3}$$

The superficial mass velocity of the gas/vapor and liquid phases are L and G, respectively.

2. Previous CFD modeling of slug flow

Computational fluid dynamics (CFD) has been recognized as a practical tool for the analysis of multiphase flow. Lun et al. (1996) used the commercial CFD to simulate the growth of a wave on the interface of two immiscible fluids with different properties in horizontal stratified gas-liquid flow (Lun, Calay & Holdo, 1996).

Anglart and Podowaski (2002) studied the fluid mechanics of Taylor bubbles and slug flow in vertical, circular channels using detailed, three dimensional CFD simulations (Anglart & Podowaski, 2002).

A series of numerical investigations on the formation and propagation of slug flows inhorizontal circular pipes have been simulated by Frank (2005).

In this article, the use of Baker chart for the prediction of flow pattern in an inclined pipeline has been examined by using CFD simulation with VOF model.

3. Slug flow characteristics

An accurate prediction of slug statistical characteristicsis required fordesigning the slug catchers and the adaptation of their safety and control system to the selected operating procedures. Dukler and Hubbard (1975) provided an insight into mechanisms of the slug formation and demonstrated that for stabilizing the slug, the rate of liquid pick up at the front of the slug must be equal to the rate of liquid shedding at the rear of it. Fig. 2 is a schematic representation of slug in a pipeline (Brill & Beggs, 1994).

In the slug flow regime, gas bubbles and liquid slugs which can contain small gas bubbles, alternately surge along the pipe. These slugs often cause operational problems, such as the flooding of downstream facilities, sever pipe corrosion, structural instability of the pipeline and wellhead pressure fluctuation (Wilkense, 1997). Kaul (1996) noted that the corrosion rate is accelerated when the flow pattern is slug flow. Since the highest corrosion rate occurs in slug flow, the ability to predict the flow regime is an important issue. Additionally, avoiding slug flow regime greatly reduces pumping cost.

The determination of the transition from stratified flow to slug flow involves the Kelvin-Helmholtz theory on wave stability. Taitel and Dukler (1976) noted that slugs appeared when a finite amplitude wave in the stratified film grew. The wave growth condition is predicted from the Kelvin-Helmholtz stability criteria. This theory is based on the thought that as gas flow over a wave flowing between plates accelerates, this acceleration causes the pressure to

decrease due to the Bernoulli Effect; therefore, the liquid level in the wave increases to oppose gravity (Taitel & Dukler, 1976)

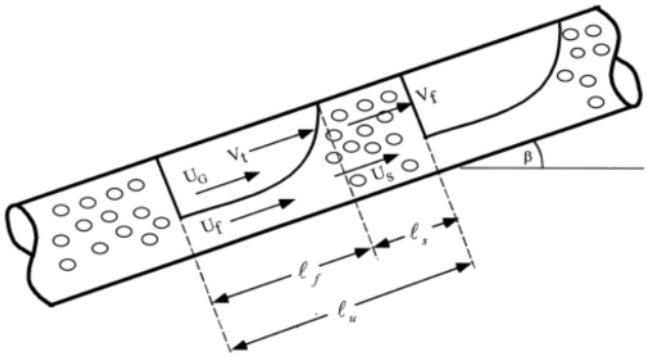

Fig. 2. Slug flow geometry

3.1 Slug length

Slug length is a significant parameter in separation facility and pipeline control. The common procedure is to find the volume of the large slugs and design a separator or slug catcher that can capture a slug of this size. In fully developed slug flow, it is convenient to define a control volume of a gas bubble and a liquid slug.

3.2 Slug transitional velocity

Slug transitional velocity in horizontal and downward inclined pipelines was investigated in this study. Slug transitional velocity is defined as the velocity of the interface between the liquid slug and gas pocket which is considered the highest velocity in a slug unit in horizontal flow.

Nicklin (1962) has suggested using Eqs. 2 to 4 for the estimation of the slug transitional velocity, V_t;

$$V_t = C_\circ V_m + V_d \tag{2}$$

$$V_d = 0.54\sqrt{gD}\cos\beta + 0.35\sqrt{gD}\sin\beta \tag{3}$$

$$V_m = V_{SL} + V_{Sg} \tag{4}$$

Where V_d is the drift velocity of the elongated bubble in a still liquid, and the mixture velocity, V_m, is equal to the sum of the liquid, V_{SL}, and gas superficial velocities, V_{Sg}. The value of $C_\circ$ is determined through experiments and is roughly equal to the ratio of the maximum velocity to the mean velocity of fully developed velocity profile. The value of $C_\circ$ equals1.2 for fully developed turbulent flow and equals2.0 for fully developed laminar flow (Taitel, Sarica & Brill, 2000). D is the pipe diameter, β is the inclination angle measured from horizontal axis and g is the acceleration of gravity.

Kuba (1990) empirical correlation seems valid for slug velocities below 15 ms^{-1} :

$$V_t = 1.21\left(0.1134 + 0.94V_{SL} + V_{Sg}\right) \quad (5)$$

In downwardly inclined pipes, the liquid film travels faster than the liquid slug mixture. As the liquid flow rate or superficial velocity, V_{LS}, increases (while the gas flow rate is constant), the liquid film hold up increases until it reaches a maximum. Hence, the tail of the slug will not shed any liquid to the film behind it because the film velocity is larger than the slug velocity (Taitel & Dukler, 1976).

3.3 Slug Frequency

The slug frequency, F_S, is equal to the total number of slugs going by a specific point along the pipeline per a certain period of time. It is a function of the inclination angle, flow rates, mean length of a slug unit and mean translational velocity. Its estimation is necessary for the exact prediction of corrosion rates.

Gregory and Scott (1969) have developed a correlation for the prediction of slug frequency, F_s. It is given by Eq. 6 and is based on a horizontal flow in 0.75 and 1.50 inch pipes.

$$F_S = 0.0226\left[\frac{V_{SL}}{gD}\left(\frac{19.75}{V_m} + V_m\right)\right]^{1.2} \quad (6)$$

Zabaras (2000) modified the Gregory and Scott (1969) correlation to include the effect of inclination angle. Zabaras equation, Eq.7, in English units is as follows.

$$F_S = 0.0226\left[\frac{V_{SL}}{gD}\left(\frac{212.6}{V_m} + V_m\right)\right]^{1.2}\left[0.836 + 2.75\sin^{0.25}(\beta)\right] \quad (7)$$

The ultimate aim of this work was to gain a deeper understanding of multiphase flow phenomena in pipeline systems and to develop guidelines to improve the design of pipelines and separation facilities such as slug catcher. In the presented work, CFD is to identify the critical parameters of slug flow, namely mean slug frequency, slug translational velocity, hold up and pressure drop.

4. CFD model

The computational fluid dynamics techniques are applied to simulate multiphase flows in a wide variety of process units. The VOF model is a surface-tracking technique applied to a fixed Eulerian mesh. It is designed for two or more immiscible fluids and can track position of the phase's interface. In the VOF model, the fluids share a single set of momentum equations, and the volume fraction of each of the fluids in each computational cell is followed throughout the domain. Segregated solver must be used while only one of the phases can be compressible. The equations being solved in the VOF model are as follows:

The volume fraction equation for the q-th phase:

$$\frac{\partial \alpha_q}{\partial t} + \bar{\upsilon}.\Delta\alpha_q = \frac{S_{\alpha_Q}}{\rho_q} \tag{8}$$

A single momentum equation is solved throughout the domain, and the resulting velocity field is shared among the phase:

$$\frac{\partial}{\partial t}(\rho\vec{\upsilon}) + \nabla.(\rho\vec{\upsilon}\vec{\upsilon}) = -\nabla p + \nabla.\left[\mu\left(\nabla\vec{\upsilon} + \nabla\vec{\upsilon}^T\right)\right] + \rho\vec{g} + \vec{F} \tag{9}$$

The density ρ and dynamic viscosity μ in the equation are dependent on the volume fraction of all phases:

$$\rho = \sum \alpha_q \rho_q \tag{10}$$

$$\mu = \sum \alpha_q \mu_q \tag{11}$$

The VOF model can also include the effects of surface tension along the interface between each pair of phases, and the contact angles between the phases and the walls can be specified (Fluent Inc., Fluent *6.3* User's Guide).

5. Simulations

5.1 Pipeline geometries and boundary conditions

The first part of the simulation work involves 2D-simulations of two-phase flow patterns for water and air. For the water- air two-phase system, six simulation cases under atmospheric pressure and at room temperature have been performed, each one chosen in the center of an operating area representing a different flow regime according to the Baker chart (Brill & Beggs, 1994). Table 1 represents flow regimes as given by Baker chart. In the first geometry, the pipeline was a pipe 7m in length and 0.08m in diameter placed horizontally. In the second geometry, the pipe line was a pipe with a length of 5m and diameter of 0.0763mplaced with inclination angles of -0.5 and -0.8 degree. The geometries are in accordance with the available experimental data (Hanratty et al., 2000).

The grids were obtained by using GAMBIT 2.3.16 which is a software for FLUENT geometry and mesh generation. For all simulations, a no-slip condition is imposed at the tube wall. The influence of the gravitational force on the flow has been taken into account. At the inlet of the tube, uniform profiles for all of the variables have been employed. A pressure outlet boundary is imposed to avoid difficulties with back flow at the outlet of the tube.

Table 1.

$G/\lambda\left(kg/\left(m^2 s\right)\right)$	$L\lambda\psi/G$	Flow Regimes from Baker chart, Fig. 1
2	2	Stratified
27	0.2	Wavy
0.2	6000	Plug
4	100	Slug
41	1000	Bubble
109	10	Spray

5.2 Solution strategy and convergence criterion

Due to the dynamic behavior of the two-phase flow, a transient simulation with time steps of 0.001, 0.0001 and 0.0005 second was employed. The calculations were carried out by the combination of PISO algorithm for pressure-velocity coupling and a second-order upwind calculation scheme for the determination of momentum and volume fraction. The convergence measure was based on the residual of calculated variables, i.e. mass, velocity components and volume fraction. In the present calculations, the numerical computations are considered converged when the scaled residuals of different variables are lowered by three orders of magnitude.

6. Results and Discussion

6.1 Flow regime observation

The simulation results for the different horizontal pipeline flow regimes are given in sections (a) to (f) of Fig. 3. The figures represent the calculated contours of mixture density in $\left(kgm^{-3}\right)$ for the different flow regimes. The mixture density is proportional to the phase composition of air and water in the tube. The red and blue colors refer to the presence of pure water and pure air, respectively. Referring to the definition of flow regimes and mixture density, the various flow regimes are distinguishable.

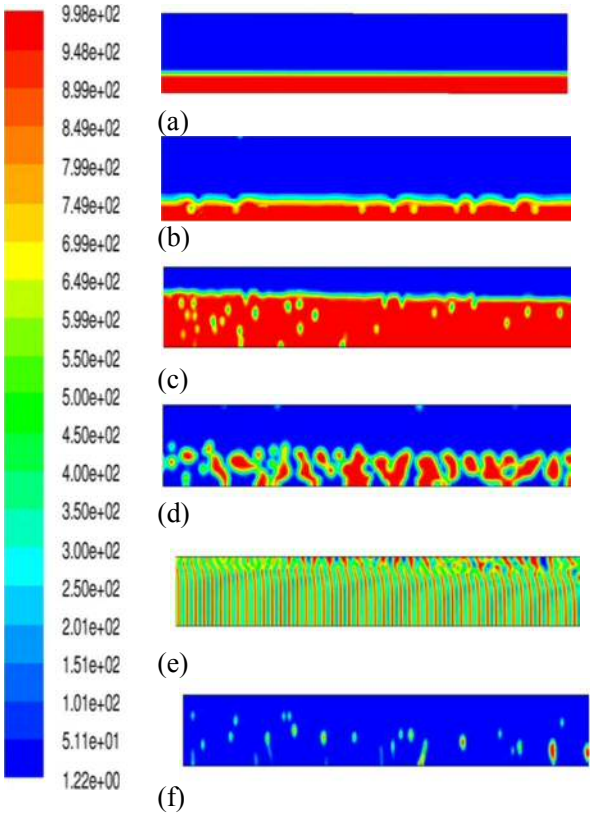

Fig. 3. Horizontal two phase flow regimes. Contours of mixture density for water-air (a) stratified flow (b) wavy flow (c) plug flow (d) slug flow (e) bubble flow (f) spray flow.

6.2 Slug length for horizontal and inclined pipelines

The changes of slug length with the experimental data at $U_{SG} = 2.4\ \left(ms^{-1}\right)$ were used for simulation. The horizontal pipe and the pipes with the slopes of -0.8 and -0.5 degree were examined. The changes of slug length at different times are clearly observable in Fig. 4. The inlet data was shown in Fig. 4 for 3 different slopes.

As it is observed in the Fig. 5, the liquid slugs appeared in the pipeline and after the passing of some time, the large liquid slugs were broken and changed to the smaller slugs and faded away after 15 seconds. In the CFD model, the rolling over and breaking of the waves, which are of slug characteristics (due to high air velocity), were observed.Fig. 5 indicates that there are instabilities on the gas liquid surface and small amplitude waves are generated. The evolved waves on the interface were not high enough to touch upper part of the tube, but by passing a short time, the liquid slugs were formed. Along the pipe length, the flow regime remained slug regime, but frequency was decreased in comparison to the first part of the pipeline.

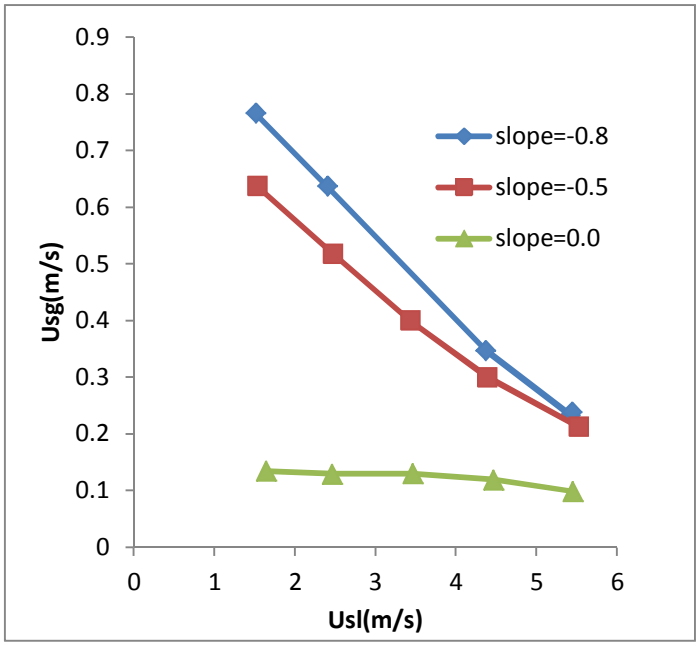

Fig. 4. The inlet data of experimental model for 3 different slopes

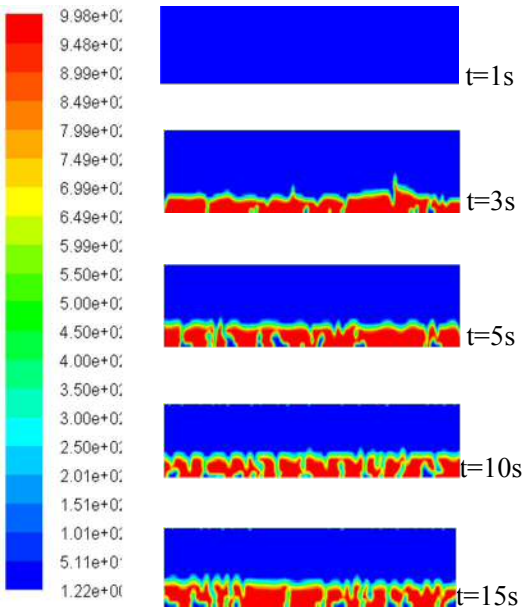

Fig. 5. The changes of slug length by passing time in the horizontal pipe

Fig. 6 shows the pipe with a slope of -0.8 degree. Increasing the pipe slope makes changes in slug's shape. The increase of gas velocity leads to the growth of waves, and soothe formation of slug. After passing about 1 second (Fig. 6 in t=6.75s), the slug breaks down. This process continues until the flow develops itself at 15 s. In negative slopes, the velocity in the tail of slug gets higher than the velocity in the front of slug. That results in slug breakage; therefore, the slug catchers are built with negative slopes to facilitate gas liquid separation.

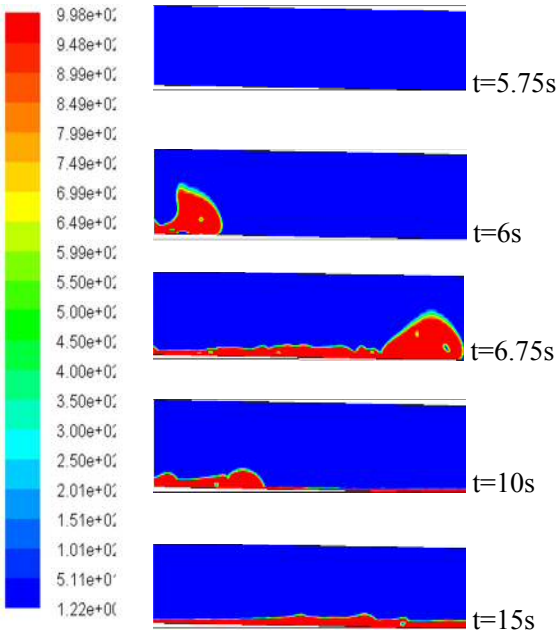

Fig. 6. The changes of slug length by passing time in pipe with $\theta = -0.8^{\circ}$

Fig. 7 shows the slug formation in the pipeline with a-0.5 degree slope. Fig.6 and Fig. 7 show that the rate of liquid hold up and slug frequency are similar for pipelines with -0.5 and -0.8 slopes.

Fig. 7 and Fig. 8 show the mechanism of slugging by CFD model and experimental approach, in a pipe with a -0.5 degree slope and in 5 steps, respectively. Hydrodynamic slugging is a mechanism that causes flow instability at the interphase of gas and liquid phases of a stratified flow. Indeed, the gas fluctuations are the main cause of instabilities. This is observed in Fig.7.There is astratified flow in second 9 of Fig.7 as the interphase of liquid–gas is smooth. In second 9.03 at the interphase, a small wave which grows in course of time is formed. The increase of gas velocity increases the partial pressure of the gas phase; therefore, the suction force reaches the interphase toward the top of the pipe and increases the wave motion exponentially. It results in the increase of the liquid height and formation of slug. At high gas velocities, the liquid height is not high enough to form slug, but uniting of roll waves is the cause of slug formation.

One of the mechanisms for the transition from stratified to slug flow is sometimes the quite slow growth of small perturbations at the gas-liquid interface due to the hydrodynamic instability of stratified flow at those conditions. The combined destabilizing effect of the Bernoulli suction force will indeed lead to the formation and growth of interfacial waves until a slug is initiated. This mechanism is well-shown on the sub figures presented in Fig. 8 which was taken from Hanratty et al. (2000). CFD simulation results as given in Fig. 7 and experimental data (Hanratty et al., 2000) of Fig. 8 are in agreement.

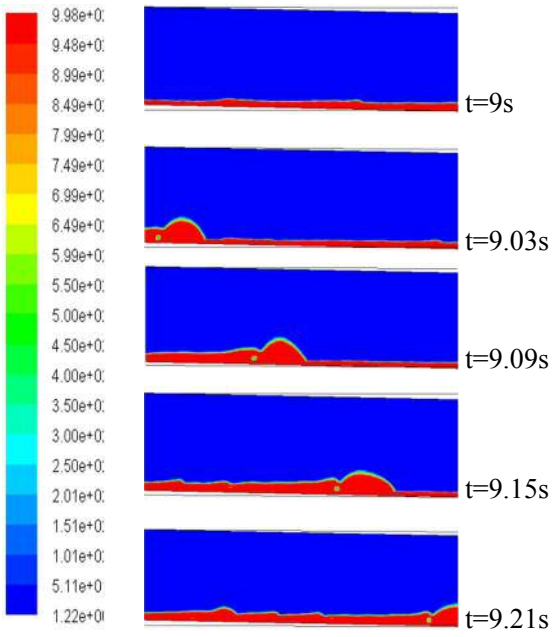

Fig. 7. Slug formation with $U_{SG} = 2/4$ (m/s) and $U_{SL} = 0.59$(m/s) $\theta = -0.5^{\circ}$

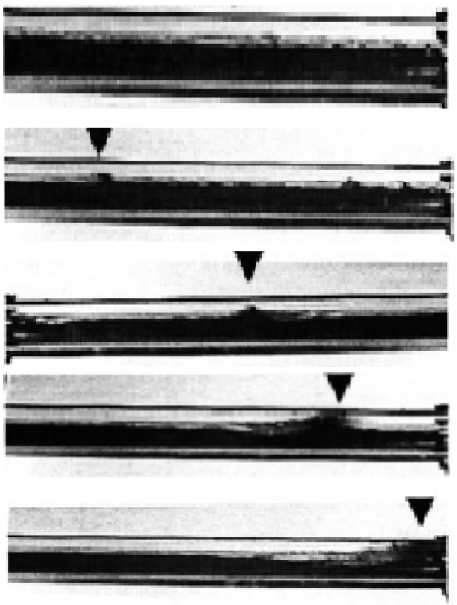

Fig. 8. Slug formation with U_{SG} =2/4 (m/s) and U_{SL} =0.59(m/s) $\theta = -0.5^{\circ}$

6.3 The effect of pipeline slope and length on the liquid hold up and slug frequency

Fig. 9 shows the mean liquid height as a function of pipe inlet condition and slope onset to slugging. To reduce computational efforts, the simulated pipeline length was 5 m. The experimental data were for a pipe length of 23 m (Hanratty et al., 2000). This is acceptable as experimental data show that the greatest changes are in the simulated range of L/D=0 to L/D= 65.5.

In Fig. 10, the experimental data of liquid hold up for a horizontal pipe (Hanratty et al., 2000) are compared with CFD model prediction. It shows that the rate of liquid hold up given by CFD model is in average 12% more than experimental data.

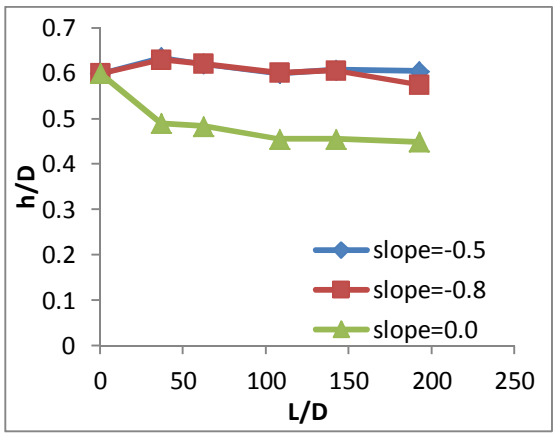

Fig. 9. The certain range for done simulations

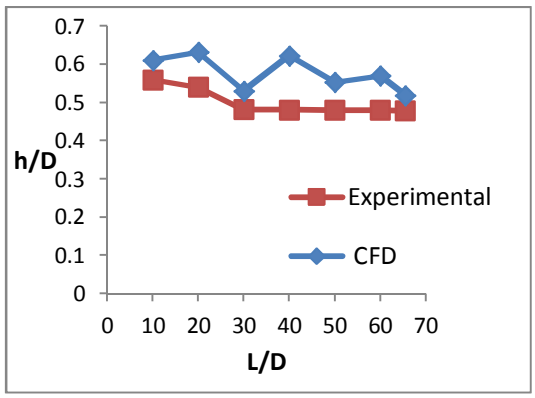

Fig. 10. The mean liquid height as a function of pipe inlet and slope onset to slugging.
$(U_{SL} = 0.14(m/s)$ and $U_{SG} = 2.4(m/s), \theta = 0.0)$

Fig. 11 and Fig.12 Showed the comparison between the experimental liquid hold up rate of -0.5 and -0.8 degree inclined pipelines (Hanratty et al., 2000) with that of CFD model.

According to Fig. 11, the rate of liquid hold up increases from L/D=0 to L/D=30. This increase continues until L/D=30 and after that, there are small changes in liquid hold up rate and the flow in pipeline has gets developed. The average differences of CFD and experimental data are about 10%.

The fluctuation in liquid hold up, Fig.12 related to the slope of -0.8 degree is comparable to the slope of-0.5 degree, Fig. 11. In this slope, too, the rate of liquid hold up increases until L/D=30 and after that it decreases. Average error between experimental data and simulation results is about 11%. In simulations, the superficial gas velocity was constant.

As it is observed, the critical liquid flow in the pipe with the slope of -0.8 degree is nearly 4 times more than the flow in the horizontal pipe. It indicates that the gravity plays a very important role in low gas velocities. It also shows, as superficial gas velocity increases, both the slope sensitivity and variation in liquid hold up in different slopes decrease (Hanratty et al., 2000).

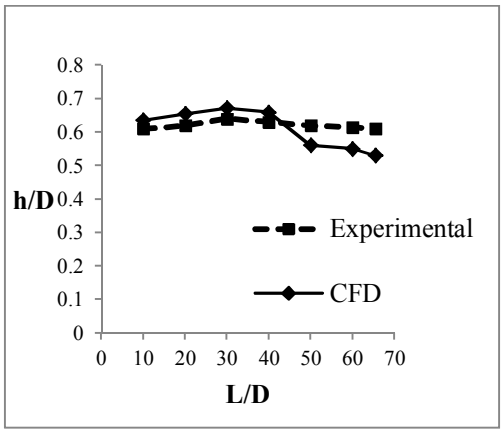

Fig. 11. The mean liquid height as a function of pipe inlet and slope onset to slugging.
$(U_{SL} = 0.53(m/s)$ and $U_{SG} = 2.4(m/s), \theta = -0.5^{\circ})$

Figs. 13, 14 and 15 show the liquid hold up fluctuation for L/D=30 and also slopes of 0.0, -0.5 and -0.8 degree in the first 10 seconds, respectively. Comparisons of Fig. 13 with Figs. 14 and 15 show that liquid holdup in horizontal pipe has more fluctuation and is more instable than the hold up in the pipes with negative slope; therefore, giving a small negative slope to the pipe highly decreases liquid fluctuation and changes the flow pattern from slug to wavy or stratified-wavy pattern.

Vertical axis in these figures represents the waves crest, and since the slug frequency is the number of passing slugs from a certain point along the pipe over the time unit, it is possible to determine the slug frequency.

Figs. 13, 14 and15 show that with decreasing the slope of the pipe from 0.0 to -0.5 and -0.8, the slug frequency decreases as slug flow changes to wavy flow. That concludesthat the slug frequency is extremely influenced by the pipe slope.

To examine the accuracy of simulation results, the data of CFD model for the horizontal pipe was extracted and the slug frequency was accounted by utilizing Zabaras correlation (Eq.7). According to simulation results and also Fig. 16,it was specified that as the pipe length increases, the slug frequency decreases.In most cases, no slug is observed at the beginning of the pipe and many slugs are formed between 10 D and 30 D and after that, the slug frequency decreases along the pipe.

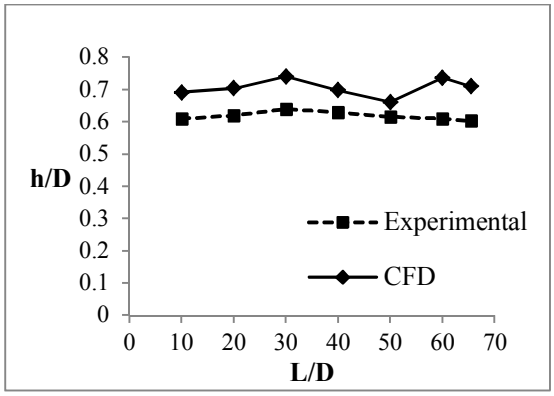

Fig. 12. The mean liquid height as a function of pipe inlet and slope onset to slugging.
$(U_{SL} = 0.53(m/s)$ and $U_{SG} = 2.4(m/s), \theta = -0.8^{\circ})$

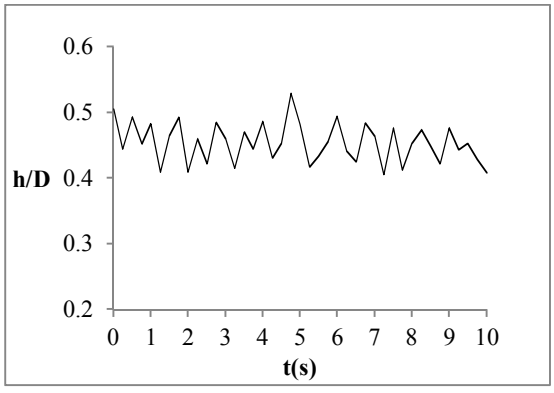

Fig. 13. The effect of slope on the liquid hold up in $L/D = 30$ and $\theta = 0.0$

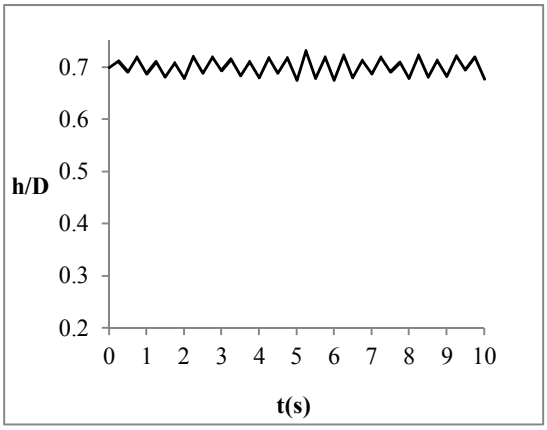

Fig.14. The effect of slope on the liquid hold up in $L/D=30$ and $\theta=-0.5^{\circ}$

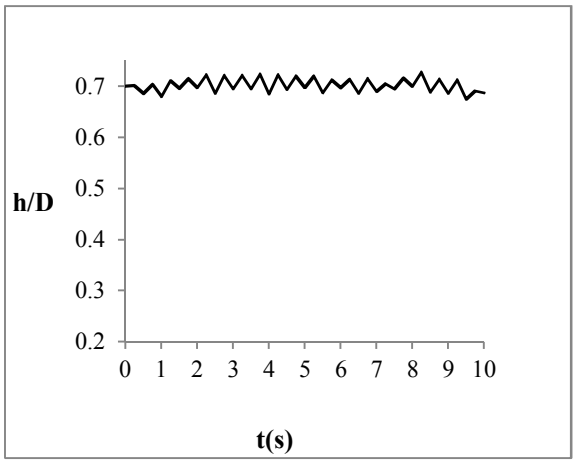

Fig. 15. The effect of slope on the liquid hold up in $L/D=30$ and $\theta=-0.8^{\circ}$

6.4 Slug translational velocity

Fig. 17 shows the correlation between slug transitional velocity and fluid mixture velocity.

In Fig. 17, slug translational velocity was accounted. As a result, the data of CFD model had a good agreement with the experimental data available in the literature and were in the same range.

6.5 Pressure drop in horizontal and inclined pipes

Fig. 18 shows the contours of absolute pressure for the horizontal pipe in second 10. As it is observed, pressure increases in parts with high liquid hold up.

Generally, the pressure drop is very high in slug flow because the liquid slugs are as obstacles for the flow of gas.

Fig. 19 and Fig. 20 show pressure gradient in a certain section (L/D=10) of the horizontal pipe and the pipes with slopes of -0.8 and -0.5 degree, respectively. It is observed that when

the slug passes from a certain section, the pressure increases. The height of picks on the figures gives the maximum pressure.

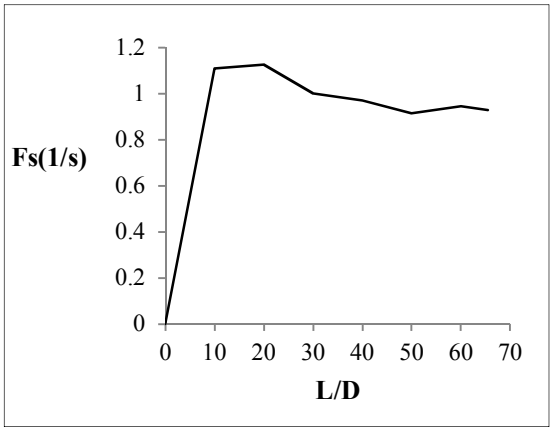

Fig. 16. Examining slug frequency along the horizontal pipeline according to Zabaras correlation

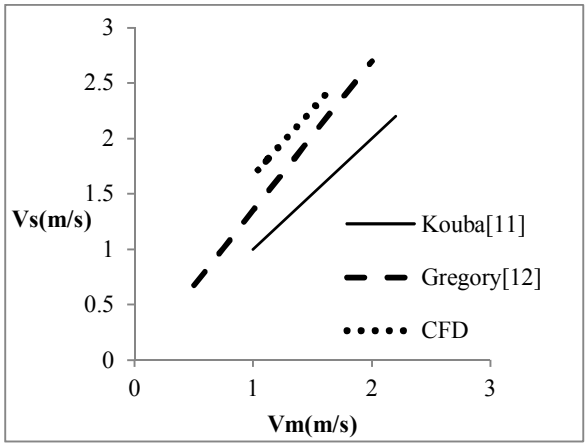

Fig. 17. The correlation between slug translational velocity and fluid mixture velocity.

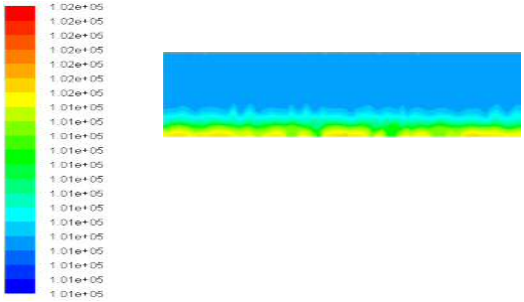

Fig. 18. The contours of absolute pressure in horizontal pipe in 10s

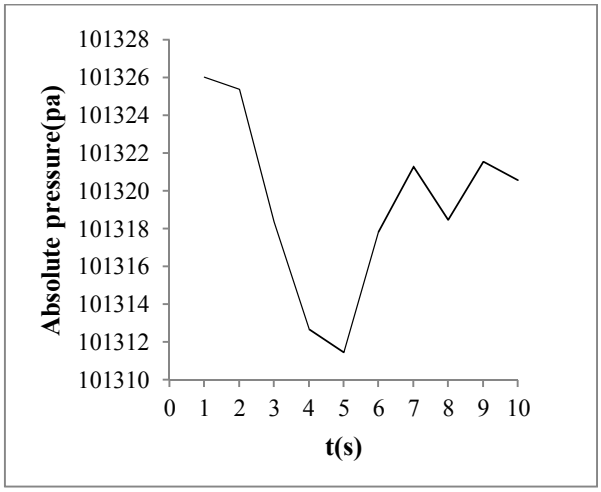

Fig. 19. Gradient pressure versus time in L/D=10 and $\theta = 0.0^{\circ}$

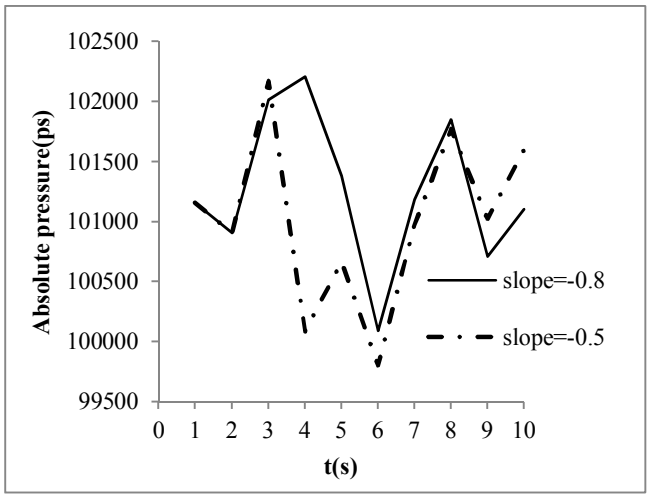

Fig. 20. Gradient pressure versus time in L/D=10 ($\theta = -0.5^{\circ}, \theta = -0.8^{\circ}$)

6.6 Slug velocity

In Fig. 21, vectors are used to show the internal structure of a slug velocity field. The color of velocity vectors shows mixture velocity in $\left(ms^{-1}\right)$. Gas moves up in slug front. A vortex effect produces fluctuation in pressure drop that was previously shown by Fig. 19.

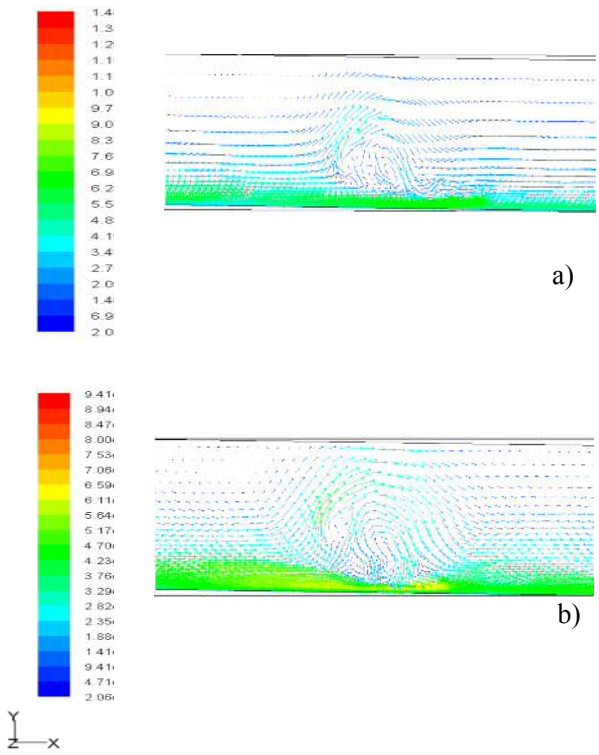

Fig. 21. Internal structure of a slug velocity field a) $\theta = 0.5^{\circ}$ b) $\theta = -0.8^{\circ}$

7. Conclusions

The CFD simulation method has the capability of improving two-phase flow modeling; therefore, CFD codes are able to calculate the different horizontal two-phase flow regimes as predicted by the Baker chart.

The VOF multiphase model is able to determine the location and geometry of the interface with accuracy. The flow regime in horizontal and inclined pipelines depends strongly on the flow rate of the inlet fluids. The analysis of the results showed that the flow structure changes significantly along the pipe for all flow regimes.

Slug flow characteristics can be adequately calculated using CFD codes. The results show that the liquid slugs do not maintain a constant length along each section and the dissipation of slugging in downward pipes mainly depends on the slug length, slug frequency and slug velocity. In the downwardly inclined pipeline, the slugs start to decay and will dissipate and their frequency will decrease. In these pipelines, stratified flow is dominant.

The simulated pressure drop and liquid hold up are comparable with the experimental data.It was concluded that VOF modeling can replace Baker chart with high generality in respect to the physical properties of gas liquid mixture, the slope of pipeline, length to diameter ratio and operating pressure.

Nomenclature

D	*Pipe diameter (m)*
C_0	*Experimental constant in equation 2*
F_S	*Slug frequency* (s^{-1})
g	*Gravitational acceleration* $\left(ms^{-2}\right)$
G	*Superficial mass velocity of the gas* $(kg(m^2 s)^{-1})$
L	*Superficial mass velocity of the liquid* $(kg(m^2 s)^{-1})$
$\vec{v}$	*Velocity vector* (ms^{-1})
V_d	*Drift velocity of elongated bubble* (ms^{-1})
Vn	*Sum of liquid and gas superficial velocity* (ms^{-1})
$Vs_{\cdot}$	*Gas superficial velocity* (ms^{-1})
$Vs_{\cdot}$	*Liquid superficial velocity* (ms^{-1})

Greek symbols

α_k	*Volume fraction of phase k*
λ	*Dimensionless parameter*
μ	*Viscosity* $\left(Pas\right)$
μ_L	*Liquid viscosity* $\left(Pas\right)$
μ_W	*Viscosity of water* $\left(Pas\right)$
ρ_l	*Liquid density* $(kg(m^3)^{-1})$
ρ_v	*Vapor density* $(kg(m^3)^{-1})$
ρ_m	*Mixture density* $(kg(m^3)^{-1})$
σ	*Gas-liquid surface tension* (Nm^{-1})
σ_w	*Water surface tension* (Nm^{-1})
ψ	*Dimensionless parameter*

References

Anglart, H., & Podowaski. (2002). Fluid mechanics of Taylor bubbles and slug flowsinvertical channels. *Nuclear science and engineering*, 140, 165-171.

Bennett, D., Woodss, Evan T., Hurlburt, Thomas J., & Hanratty. (2000). Mechanism of slug formation in downwardly inclined pipes. *International Journal of Multiphase Flow*, 24, 977-998.

Brill, J., & Beggs, H. (1994). *Two phase flow in pipes (6 th ed.)*. University of Tulsa Press.

Dukler, A.E., & Hubbard, M.G. (1975). A model for gas-liquid slug flow in horizontal and near horizontal tubes. *Ind. Eng. Chem. Fund*, 14, 337-347.

Eissa Al–Safran. (2009). Investigation and prediction of slug frequency in gas/liquid horizontal pipe flow. *Journal of Petroleum Science and Engineering,* 69, 143-155.

Fluent Inc., Fluent *6.3* User's Guide.

Frank, T. (2005). Numerical simulation of slug flow regime for an air- water two- phase flow in horizontal pipes. *The International Topical Meeting on Nuclear Reactor Thermal-Hydraulics,* 2-6.

Gregory, G., & Scott, D. (1969). Correlation of liquid slug velocity and frequency in horizontal co-current gas-liquid slug flow. *AIChE J,* 15(6), 933-935.

Kaul & Ashwini. (1996). *Study of slug flow characteristics and performance of corrosion inhibitors, in multiphase flow, in horizontal oil and gas pipelines* (MSc Theses), Ohio University.

Kouba, G.E., & Jepson, W.P. (1990). The flow of slugs in horizontal and two phase pipelines, Trans. *ASME,* 112, 10-24.

Lun, I., Calay, R. K., & Holdo, A. E. (1996). Modelling two- phases flows using CFD, *Applied Energy,* 53, 299-314.

Nicklin, D,J. (1962). Two phase bubble flow. *Chem. Eng.Sci*.,17, 693-702.

Sandra, C.K. De Schepper., Geraldine J, Heyderickx., Guy B, Marin. (2008). CFD modeling of all gas–liquid and vapor–liquid flow regimes predicted by the Baker chart, *Chemical Engineering Journal,* 138, 349-357.

Taitel, Y., & Dukler, A. E. (1976). A model for prediction flow regime transitions in horizontal and near horizontal gas-liquid flow, *AIChE Journal,* 22

Taitel, Y., Sarica, C., & Brill, J.P. (2000). Slug flow modeling for downward inclined pipe flow: theoretical considerations. *International Journal of Multiphase flow*, 26, 833-844.

Wilkense, R. J. (1997). Prediction of the flow regime transitions in high pressure, large diameter, inclined multiphase pipelines.; Ohio University

Zabaras, G. (2000). Prediction of slug frequency for gas/liquid flows, SPE 65093. SPEJ, 5(3).